Vol. 8(30), Oct. 2018, PP. 3975-3987

Contents list available at IJMEC

International Journal of Mechatronics, Electrical and Computer Technology (IJMEC)

Journal Homepage: www.aeuso.org

PISSN: 2411-6173 - EISSN: 2305-0543

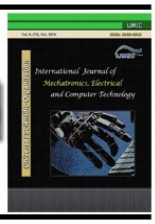

Using Model Predictive Current Control with Duty Cycle Optimization to Control Three-Phase Grid-Tied Inverter

Shahrouz Ebrahimpanah[1,*], Misbawu Adam[1, 2], Qihong Chen[1], Yuepeng Chen[1]

[1]*School of Automation, Wuhan University of Technology, 430070, Wuhan, China.*

[2]*Department of Electrical/Electronic Engineering Kumasi Technical University, P.O. Box 854, Kumasi, Ghana*

***Corresponding Author's E-mail:** shahrooz6485@yahoo.com*

Abstract

This paper proposes a model predictive current control (MPCC) for a two-level three-phase inverter with output LC filter connected to the grid by using a duty cycle Optimization by using Forward Euler approximation. The prior control methods achieve good steady-state and dynamic performance. To achieve much better steady state performance, in the prior model predictive current control (MPCC), the discrete-time system model is used to check each of the 7 possible switching states to choose a state that minimizes the cost function, which is related to the current errors. However, single voltage vector employed in one control period is extremely limited to decrease the current ripples to a minimum value. Hence, to obtain sufficient performance, the sampling frequency is necessary to choose high. In order to resolve this issue, a duty ratio optimization technique has been performed by designating one nonzero vector and the rest time for a zero vector during one control period. Simulation verify that, compared to the prior method, the proposed method (The proposed MPCC) obtain much better steady-state a reduced current ripples and total harmonic distortion(THD).

Keywords: *Model predictive current control, Duty cycle, Cost function, Voltage vector selection, Three-phase Grid-Tied Inverter.*

1. Introduction

Based on the EIA[1]'s International Energy Outlook released in 2013, the world energy consumption will become larger by 56% between 2010 and 2040, and the renewable technologies, especially wind and solar, will be increasingly added to the power grid as the new generating capacity [11], [2]. In recent years, the use of Grid-connected Power Converters has become very common in various applications as an example of the integration of renewable energy sources and motor drives. And three-phase inverters play a key role for a wide range of systems. Hence, the process of creating a new method in control strategies for this special type of power converters has pulled toward the concern of both academic and industry researchers more and more [9]. In the recent decades, different kinds of control strategies have been presented. One of those is predictive control, which is known as a fascinating choice for the control of power converters due to its fast dynamic response. Model Predictive Control (MPC) is introduced under the name of predictive control [7] and can be sorted into two groups: Continuous Control Set MPC (CCSMPC) and Finite Control Set MPC (FCSMPC) also called Discrete MPC [16]. Some advantages of this Controller (MPC) can be expressed as: easy concepts, constraints and nonlinearities of the system make it to be easily used, and the expected behavior of

[1] International Energy Agency

Article History:
Received Date: Jul. 09, 2018
Accepted Date: Sep. 03, 2018
Available Online: Oct. 01, 2018

the system is expressed as a cost function to be minimized [4]. Nowadays, the Current control is playing a key role in the control of different kinds of power converters. One of the most popular control methods for the current control is Predictive Current Control (PCC) [8].

This paper presents a Model Predictive Current Control (MPCC) with optimal duty cycle based on Forward Euler approximation, for grid-connected three-phase inverter with output LCL filter, and it can meaningfully be established a better steady state performance with the meaning of less currant harmonics and lower power ripples in the recommended Model Predictive Current Control (MPCC with optimal duty cycle). From the other point of view, to have no affection on the dynamic response and obtain much better steady state performance we need to use both a non-zero voltage vector and a zero voltage vector during one control period, where the non-zero vector is reached from customary MPCC and the period of time of the non-zero vector will be found according to reducing the current error in the end of next control period [12], [14], [15], [16]. This paper is organized as follows: Section II introduces the model of three-phase inverter with output LCL filter. Next, principle of MPCC is proposed in section III. Then, principle of MPCC with optimization of duty cycle is surveyed for Forward Euler approximation in section IV. And in section V, Simulation and Experiment will be carried out. Finally, some conclusions are summed up in Section VI.

2. Model of three-phase inverter with output LCL filter

2.1. Converter model

Fig. 1 shows the electrical scheme of a two-level three-phase inverter with output LCL filter connected to the grid. The three-phase inverter has six power switches referred to as S_x where $x = 1, \dots, 6$ and this leads to seven different, possible combinations of the switching states. Additionally there is an LCL filter connected to the RL-load and grid.

The switching state of the six power switches can be symbolized by the switching signals S_a, S_b, and S_c determined as follows [7].

$$S_a = \begin{cases} 1 \text{ if } S_1 \text{ on and } S_4 \text{ off} \\ 0 \text{ if } S_1 \text{ off and } S_4 \text{ on} \end{cases} \quad (1)$$

$$S_b = \begin{cases} 1 \text{ if } S_2 \text{ on and } S_5 \text{ off} \\ 0 \text{ if } S_2 \text{ off and } S_5 \text{ on} \end{cases} \quad (2)$$

$$S_c = \begin{cases} 1 \text{ if } S_3 \text{ on and } S_6 \text{ off} \\ 0 \text{ if } S_3 \text{ off and } S_6 \text{ on} \end{cases} \quad (3)$$

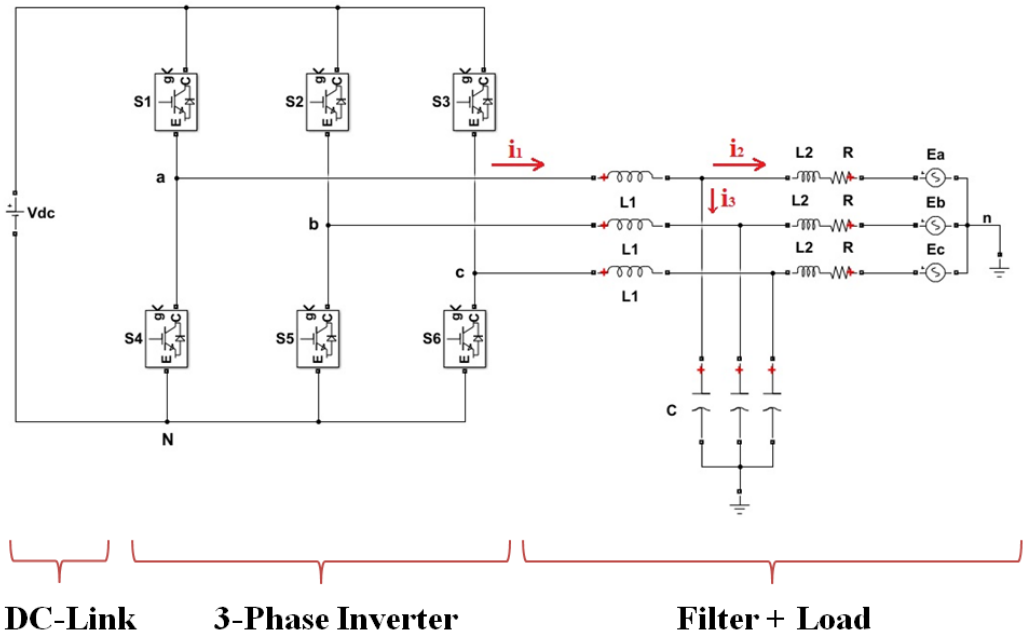

Figure 1. Topology of a two-level three-phase inverter with output *LCL* filter.

And the switching state vector can be defined by,

$$S = \frac{2}{3}(S_a + aS_b + a^2S_c) \tag{4}$$

where: $a=e^{j\frac{2\pi}{3}} = -\frac{1}{2} + j\frac{\sqrt{3}}{2}$, which represents the 120° phase displacement between the phases, So the output voltage vector can be expressed by,

$$\mathrm{V} = \frac{2}{3}(\mathrm{V_{aN}} + \mathrm{aV_{bN}} + \mathrm{a^2V_{cN}}) \tag{5}$$

where V_{aN}, V_{bN}, and V_{cN} are the phase-to-neutral (N) voltages of the inverter. And (N) is the negative terminal of the DC-link (see Fig. 1) [7].

$$V_{aN} = S_aV_{dc} \tag{6}$$

$$V_{bN} = S_bV_{dc} \tag{7}$$

$$V_{cN} = S_cV_{dc} \tag{8}$$

So it can be expressed, output voltage vector V can be having a relationship with the switching state vector S by,

$$V = V_{dc}S \tag{9}$$

Where, V_{dc} is the DC source voltage, and line to line voltage vector $[Vab \quad Vbc \quad Vca]^T$can be expressed by the following,

$$\begin{bmatrix}\mathrm{V_{ab}}\\ \mathrm{V_{bc}}\\ \mathrm{V_{ca}}\end{bmatrix} = \mathrm{V_{dc}}\begin{bmatrix}1 & -1 & 0\\ 0 & 1 & -1\\ -1 & 0 & 1\end{bmatrix}\begin{bmatrix}\mathrm{S_a}\\ \mathrm{S_b}\\ \mathrm{S_c}\end{bmatrix} \tag{10}$$

According to all the possible combinations of the gating signals S_a, S_b, and S_c, eight switching states and consequently eight voltage vectors are achieved, because of $V_0 = V_7$, so there is only seven different voltage vectors can be seen as a result (see Table 1) [4].

Table 1: Switching states and voltage vectors

#	Switching Vectors			Line to Neutral (N) Voltage			Line to Line Voltage			Voltage vector
	S_a	S_b	S_c	V_{aN}	V_{bN}	V_{cN}	V_{ab}	V_{bc}	V_{ca}	
0	0	0	0	0	0	0	0	0	0	$V_0 = 0$
1	1	0	0	V_{dc}	0	0	V_{dc}	0	$-V_{dc}$	$V_1 = \frac{2}{3} V_{dc}$
2	1	1	0	V_{dc}	V_{dc}	0	0	V_{dc}	$-V_{dc}$	$V_2 = \frac{1}{3} V_{dc} + j\frac{\sqrt{3}}{3} V_{dc}$
3	0	1	0	0	V_{dc}	0	$-V_{dc}$	V_{dc}	0	$V_3 = -\frac{1}{3} V_{dc} + j\frac{\sqrt{3}}{3} V_{dc}$
4	0	1	1	0	V_{dc}	V_{dc}	$-V_{dc}$	0	V_{dc}	$V_4 = -\frac{2}{3} V_{dc}$
5	0	0	1	0	0	V_{dc}	0	$-V_{dc}$	V_{dc}	$V_5 = -\frac{1}{3} V_{dc} - j\frac{\sqrt{3}}{3} V_{dc}$
6	1	0	1	V_{dc}	0	V_{dc}	V_{dc}	$-V_{dc}$	0	$V_6 = \frac{1}{3} V_{dc} - j\frac{\sqrt{3}}{3} V_{dc}$
7	1	1	1	V_{dc}	V_{dc}	V_{dc}	0	0	0	$V_7 = 0$

2.2. Load model

Since the impedance of C is relatively large in comparison to the impedance of the L1 and L2, the current through C can be ignored [10]. So it can be defined by,

$$i_3 = 0, i_1 = i_2 = i \tag{11}$$

For each phase, grid side current dynamics can be written as,

$$\begin{cases} V_{an} = L\frac{di_a}{dt} + Ri_a + e_a \\ V_{bn} = L\frac{di_b}{dt} + Ri_b + e_b \\ V_{cn} = L\frac{di_c}{dt} + Ri_c + e_c \end{cases} \tag{12}$$

where: R is the load resistance and $L = L_1 + L_2$.
By replacing (12) into (5), a vector equation for the grid side current dynamics can be achieved by,

$$V = L\frac{d(^2/_3(i_a+ai_b+a^2i_c))}{dt} + R(^2/_3(i_a + ai_b + a^2i_c)) + {}^2/_3(e_a + ae_b + a^2e_c) \tag{13}$$

where: $a = e^{j\frac{2\pi}{3}} = -\frac{1}{2} + j\frac{\sqrt{3}}{2}$, $i = {}^2/_3(i_a + ai_b + a^2i_c)$ and $e = {}^2/_3(e_a + ae_b + a^2e_c$.Hence, the grid side current dynamics can be expressed by the vector differential equation,

$$V = L\frac{di}{dt} + Ri + e \tag{14}$$

where V is the voltage vector generated by the inverter, i is the grid side current vector, and *e* grid side voltage vector [4].

3. Principle of MPCC

In a conceptual manner, the proposed predictive control strategy is based on the fact that the system needs to select the appropriate switching state according to minimization of the cost function. Hence, at the present time the Model Predictive Current Control is a new access to the non-linear current control in three-phase inverters [6].

3.1. Discrete-time model for prediction

A discrete-time equation to predict the future value of load current is achieved by using the forward Euler approximation to obtain a discrete-time system representation. The discrete-time model can be acquired by using the simple derivative approximation [3]. The derived approximation is given by,

$$\dot{x} \approx \frac{x(k+1)-x(k)}{T_{sp}} \tag{15}$$

where T_{sp} the sampling period, k is for sampling of the present time; and x is the state variable. The grid side current derivative $\frac{di}{dt}$ is substituted for the Forward Euler approximation [3]. In other words, the derivative is approximated as follows.

$$\frac{di}{dt} \approx \frac{i(k+1)-i(k)}{T_{sp}} \tag{16}$$

Based on equation (14), the differentiation of grid current can be determined as follows,

$$\frac{di}{dt} = \frac{V-e-Ri}{L} \tag{17}$$

Therefore, by replacing (17) into (16), predictions of the future load current at time (k + 1) for various values of voltage vector V_k can be obtained as follows [3], [4].

$$i(k+1) = i(k) + \frac{T_{sp}}{L}[V(k) - e(k) - Ri(k)] \tag{18}$$

3.2. Cost function

As shown in Fig. 2, the cost function needs the predicted output currents $i(k+1)$. As the controller is shown in Fig. 2, it can use any allowed output to bring the controlled currents closer to their reference current. The future value of the grid side current, $i(k+1)$, is predicted for the 7 permissible switching states generated by the inverter. For this objective, it is necessary to have the prevailing grid side current. Hence, it should be measured. After obtaining the predictions, a cost function (g) as shown in the Equation (19), is appraised for each switching state. The goal of the current control scheme is to reduce as much as possible the errors between the reference currents and the measured values. The above-mentioned necessity can be shown in the form of a cost function. Therefore in the next sampling period, the switching state (and so the voltage vector generated by the two-level three-phase inverter) that minimizes g, is chosen and applied. And if g = 0, the reference current equals with its output current. So, the purpose of this Optimization Cost Function is to obtain g value as close as possible to zero. Then, the voltage vector that minimizes the cost function is selected and put at the next sampling instant [1], [3].

$$g = f(i_{ref}(k+1), i(k+1)) \tag{19}$$

The cost function can be defined in absolute value terms by measuring the error between the references and the predicted currents.

$$g = \left|Re[i_{ref} - i(k+1)]\right| + \left|Im[i_{ref} - i(k+1)]\right| \tag{20}$$

where $i(k+1)$ is predicted from equation (18) and i_{ref} is expressed from,

$$i_{ref} = \frac{2}{3}(i_{a-ref} + ai_{b-ref} + a^2 i_{c-ref}) \tag{21}$$

where i_{a-ref}, i_{a-ref} and i_{a-ref} are the reference current vector for phase a, b and c, which are generated by Sine Wave Creator with the 120° phase displacement. The main goal of the cost function in equation (20) is to decrease the output current error. And at last the best voltage vector can be determined as follow,

$$V_{opt} = V(min\{g_n\}) \quad (n = 0,1,2,\dots,7) \tag{22}$$

where g_n is the cost function for various possible switching and $\mathrm{V}(\min\{g_n\})$ is known as the voltage vector with optimum cost function.

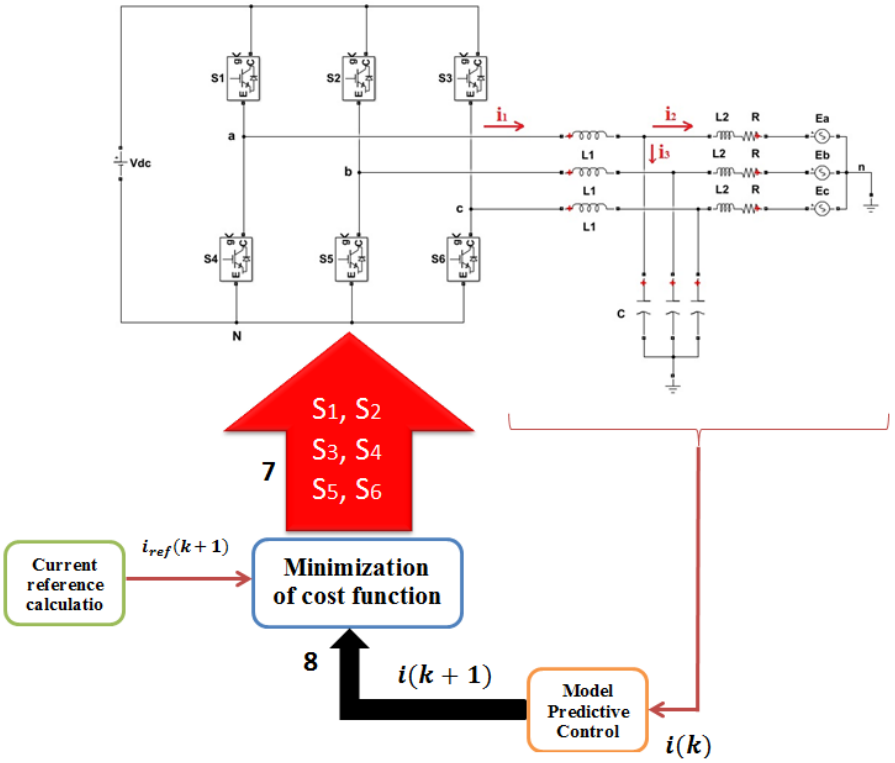

Figure 2. Control diagram of Two-level three-phase inverter with output *LCL* filter connected to the grid.

4. Principle of MPCC with optimization of duty cycle

During one control period in routine MPCC, there is only one voltage vector that can be chosen and applied. And it is a reason for some disadvantages, as an example power ripples greater than normal, which restrict the steady-state performance and have more current harmonics. In order to facing up to these problems, we need to use a new method (MPCC with optimization of duty cycle), that is to say, an appropriate zero voltage vector and a non-zero voltage vector should be applied during one control cycle [15]. Hence, it can be done to use the combination of a non-zero voltage vector and a zero voltage vector during one control cycle to decrease the errors between the reference value and the measured value of grid side current at the end of the next control cycle [12].

4.1. Vector selection

In the MPCC with optimization of duty cycle control, the control period will be divided into a non-zero and zero voltage vector. At this method, the best voltage vector minimization can be chosen at the next control period as well according to equation (20). However, it is important to know that, because a zero vector has already been chosen as one of the two vectors for the MPCC with optimal duty cycle control, then if the best voltage vector was a zero vector, a suboptimal vector should be chosen in place of the zero vectors. This is due to the fact that only one zero and one non-zero can be selected during one control period. And to have a better result, it is preferable to combine a suboptimal vector with a zero vector instead of using zero vectors only during one control period [15]. Therefore, the best voltage vector (the non- zero voltage vector with minimum cost function) can be obtained as follows,

$$V_{n-z} = V(min\{g_n\}) \quad (n = 1,2,\dots,6) \tag{23}$$

where $\mathrm{V}(\min\{g_n\})$ is the only voltage vector with optimum cost function among non- zero vectors.

4.2. Optimal duty ratio

Due to combination of the zero voltage and the non-zero voltage vectors during one control period, only six non-zero voltage vectors can be used to predict the next moment value of the grid side current in (20). By definition of the slopes of grid side current for the zero and the non-zero voltage vectors which can be obtained easily from (17), the duration of the non-zero voltage vector can be determined [16]. Hence it can be expressed by,

$$s_1 = \frac{V_{n-z} - e - Ri}{L} \tag{24}$$

$$s_0 = \frac{-e - Ri}{L} \tag{25}$$

where s_0 and s_1 are the slopes of grid current for the zero voltage vector and the non- zero voltage vector, respectively. And V_{n-z} is the best non- zero voltage vector. From this place, according to equation (18), the current at the end of the next control period can be calculated as,

$$i^o(k+1) = i(k) + \frac{T_{opt}[V_{n-z} - e(k) - Ri(k)] + T_z[V_z - e(k) - Ri(k)]}{L} \tag{26}$$

$$T_{opt} + T_z = T_{sp} \tag{27}$$

$$V_{n-z} + V_z = V_k \tag{28}$$

where $T_{opt}\ and\ T_z$ are the optimal duration of the non-zero and zero voltage vectors, respectively. V_{n-z} is the best non- zero voltage vector and V_z, zero voltage vector where is equaled zero. Then, by substituting (24) and (25) into (26) the current at the end of the next control period can be achieved by,

$$i^o(k+1) = i(k) + s_1 \times T_{opt} + s_0 \times (T_{sp} - T_{opt}) \tag{29}$$

It is necessary to know how long the non-zero vector should be employed during one control period. In this paper, the optimal duration of T_{opt} can be achieved based on the deadbeat control theory, the current at $(k+1)th$ instant should reach its reference value i_{ref} when the selected voltage vector V_k is applied for a fraction of control period. To obtain this goal, the following equation should be determined,

$$i^o(k+1) = i_{ref} \tag{30}$$

$$i_{ref} = i(k) + s_1 \times T_{opt} + s_0 \times (T_{sp} - T_{opt}) \tag{31}$$

Solving (30), the optimal duration for the non-zero vector can be obtained as,

$$T_{opt} = \frac{\left|i_{ref} - i(k) - s_0 \times T_{sp}\right|}{|s_1 - s_0|} \tag{32}$$

It is important to pay attention that the value of T_{opt} can be saturated to zero only if T_{opt} is less than zero, and T_{opt} is more than T_{sp}, then it will be saturated to T_{sp}[16].

4.3. Vector sequence

The impact of the switching frequency should be considered because of the loss of switch. Hence, the two outlooks should be concerned to have less switching frequency. Firstly, the non-zero vector will be employed, in this situation, and it should be chosen an appropriate zero vector to present the minimal switching jumps. For example, if the voltage vector “100” is selected as the non-zero voltage vector, the appropriate zero voltage vector will be chosen as “000” rather than “111.” Secondly, if the previous vector sequence includes the same zero vector, the zero vector will be applied first to achieve minimal jumps between the adjoining vector sequences. Such as, if the vectors during the last period are “110” and “111” with “111” at the end, and the vectors to be applied in the next period are “011” and “111,” in that case, “111” instead of “011” will be applied first to reduce the switching frequency [14].

4.4. Control digital delay compensation

In a real-time performing, the delay caused by digital processing will spoil the performance of MPCC. Therefore, the digital processing delay should be noted and compensated in order to achieve the excellent prediction accuracy [13]. To remove this delay, the value at the $(k\ +\ 2)^{th}$ instant should be used in (20) and not the $(k\ +\ 1)^{th}$ instant, which needs a two-step prediction [5]. Due to that, the cost function in (20) will be replaced as follows,

$$g = \left|Re[i_{ref}\ - i(k+2)]\right| + \left|Im[i_{ref}\ - i(k+2)]\right| \tag{33}$$

where $i(k+2)$ is predicted from $i(k+1)$, which can be determined as follows,

$$i(k+2) = i(k+1) + \frac{T_{sp}}{L}[V(k+1) - e(k+1) - Ri(k+1)] \tag{34}$$

4.4. The implementation diagram

In Fig. 3 a flow diagram of how the predictive algorithm is implemented for the two-level three-phase inverter is illustrated. In general, the control algorithm can be expressed by the following steps:

1) The grid side current and DC-link voltage are measured.
2) The value of the optimum cost function is initialized.
3) The grid side current is predicted for the next sampling instant (for the entire non-zero vectors).
4) Evaluating the cost function for each prediction.
5) Choosing the optimal switching state according to the optimum cost function.
6) Finding the slopes of grid side current for the non-zero voltage vector and the zero voltage vectors.
7) Duty Cycle is determined.
8) Applying the new switching state according to optimal Duty Ratio.

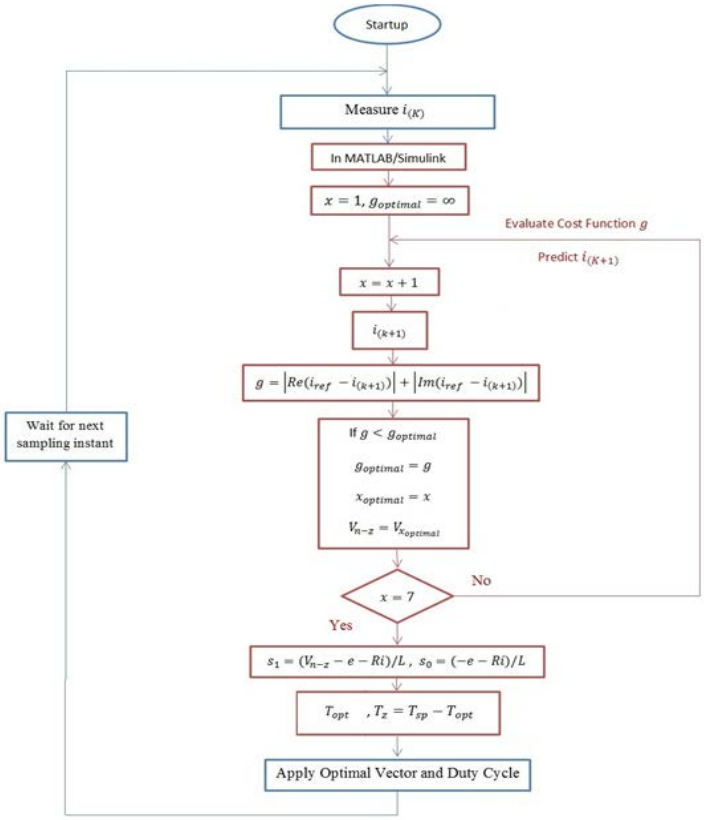

Figure 3. Flow diagram of MPCC with optimization of duty cycle.

5. Simulation

To verify the performance of the proposed MPCC with optimal duty cycle, simulation model and several experiments of a two-level three-phase inverter with output LCL filter connected to the grid with the system and control parameters as indicated in Table 2 has been developed. The results of the prior MPCC will be achieved for the purpose of comparison. Generally, simulation diagram of the prior MPCC and the proposed MPCC with duty cycle optimization is presented in Fig.4.

Table 2: Parameters used for the simulations

Variable	System Parameters	Value
V_{dc}	DC-Link voltage	700V
R	Internal resistance	1Ω
e	Grid Voltage (RMS)	220V
f	Line voltage frequency	50Hz
i_{ref}	Reference current peak amplitude	40A
L_2	Filter inductance	1mH
L_1	Filter Inductance	3mH
C_f	Filter Capacitance	5μF
R_f	Filter Resistance	20Ω
T_{sp}	Sampling time	50μs

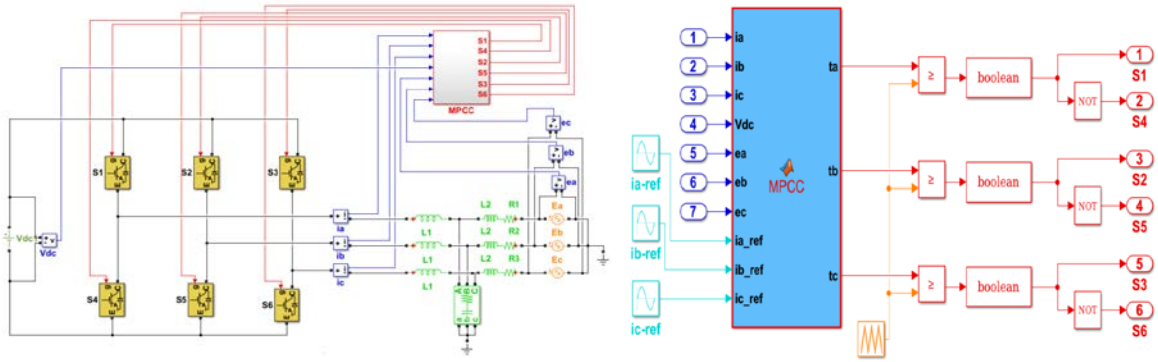

(a) (b)

Figure 4. Simulation diagram of inverter in MATLAB/Simulink. (a) Predictive current control technique for a two-level three-phase inverter with output *LCL* filter connected to the grid. (b) Subsystem of the MPCC.

Simulations of a three-phase inverter have been done with MATLAB/Simulink, in order that estimate the performance of the proposed predictive strategy, compared with the conventional scheme.

By comparing these two kinds of method, prior MPCC and proposed MPCC with optimal duty cycle control, it can see clearly that the distortion of output current in proposed MPCC with optimal duty cycle control is much less than prior MPCC method and presents less current ripples and lower current harmonics. Fig. 5 shows the grid side current for prior and proposed MPCC of a two-level three-phase inverter with output LCL filter.

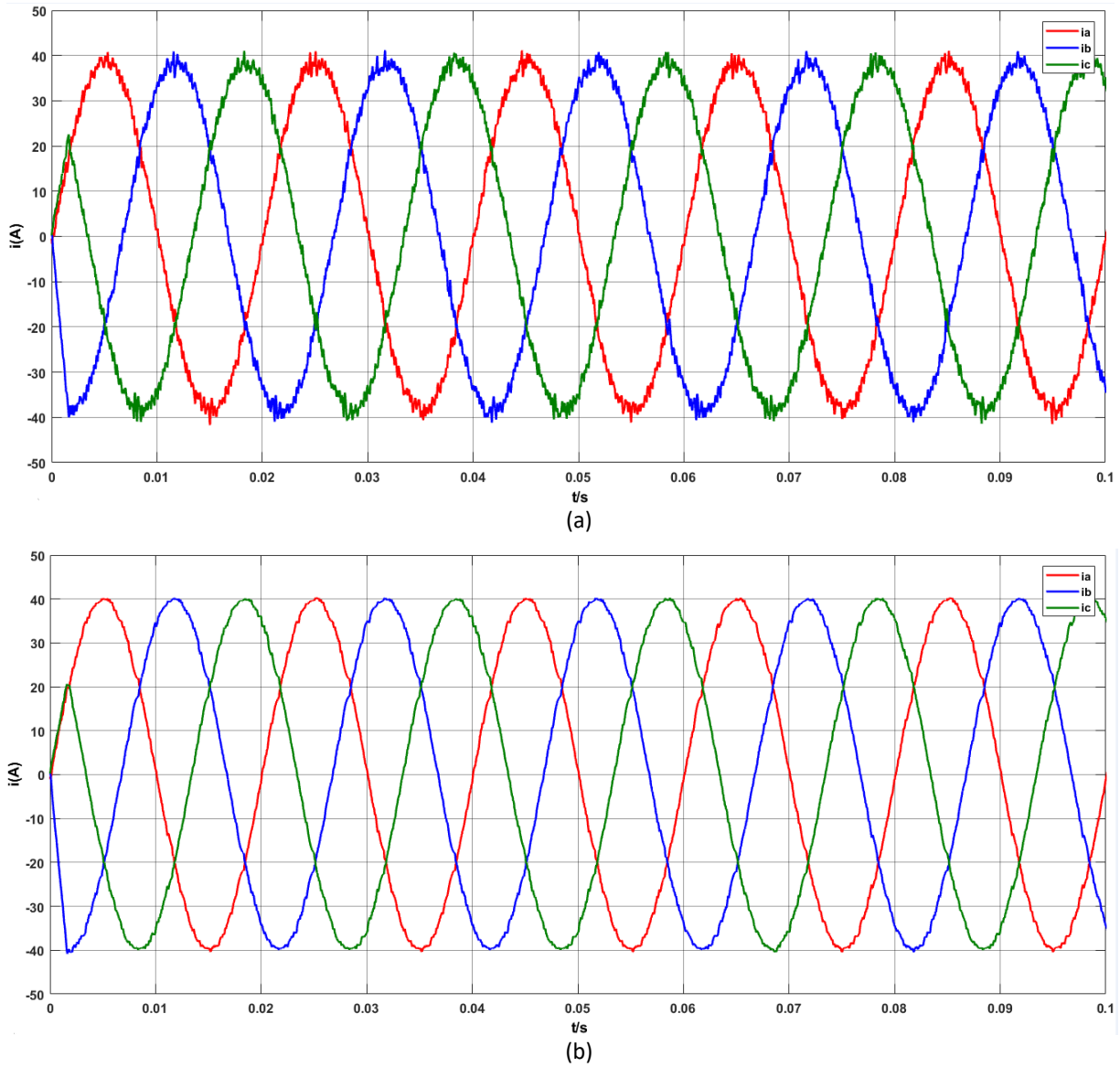

Figure 5. Simulation waveform of three phase grid current at 50μs sampling time for (a) the prior MPCC and (b) the proposed MPCC with optimal duty cycle control.

As it can clearly be seen the current THD of the proposed MPCC is 1.6%, much better than 3.69% of the prior MPCC. Fig. 6 represents the harmonic spectrum analysis at different control strategies. Therefore, the current waveforms are more closed to sinusoidal which the efficiency of proposed MPCC with optimal duty cycle control at making better steady-state performance will be confirmed.

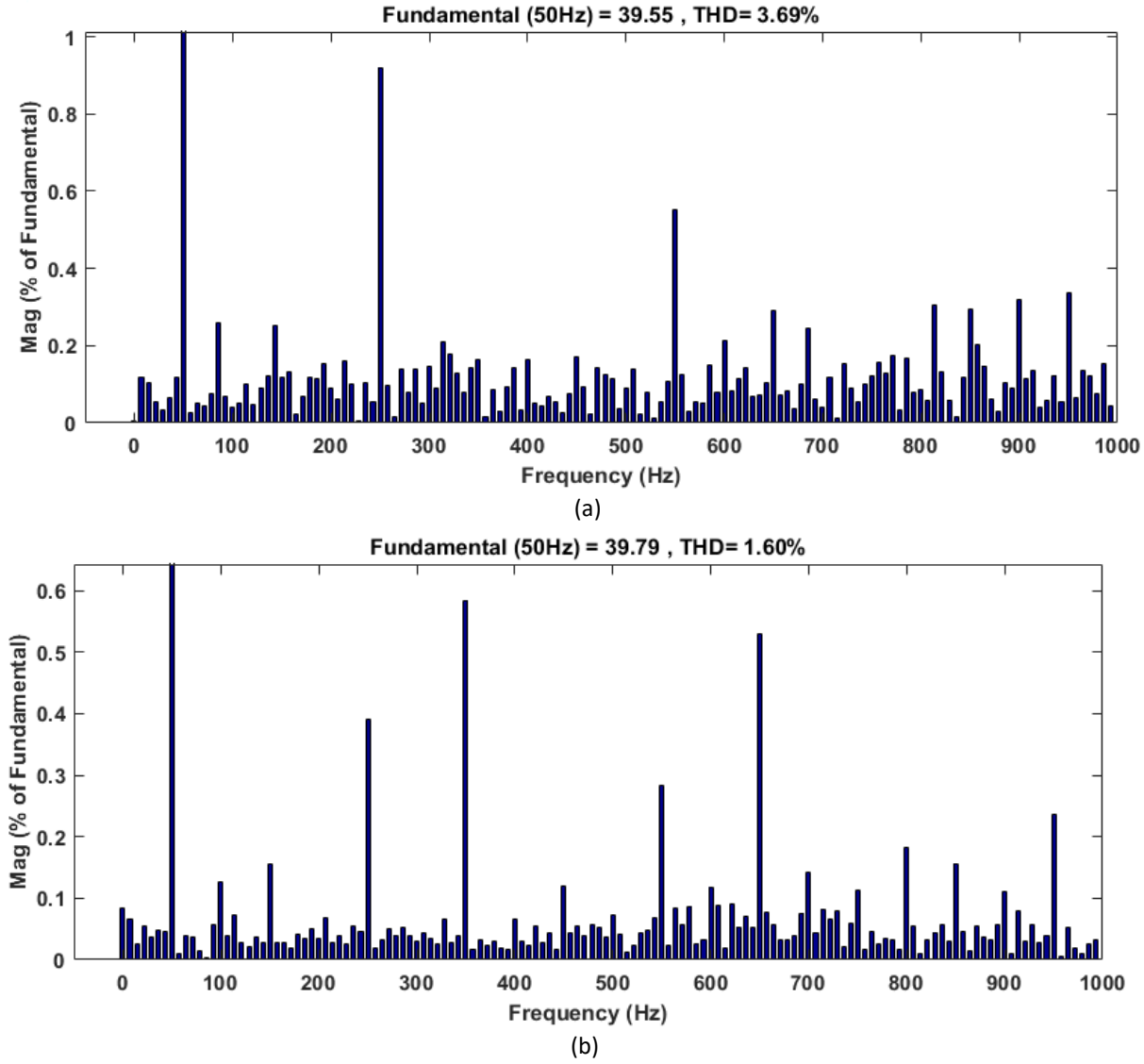

Figure 6. Harmonic spectrum of grid side current at 50μs sampling time for (a) the prior MPCC and (b) the proposed MPCC with optimal duty cycle control.

Conclusion

The MPCC with optimal duty cycle control by using Forward Euler method for a two-level three-phase inverter with output LCL filter has been presented in this paper. The Implementation diagram checks each of the 7 possible switching states to choose a state that minimizes the cost function. To obtain much better steady state performance, the proposed MPCC is required to employ one zero vector and one nonzero vector during one control period. The idea of duty cycle optimization is also proposed to achieve steady state performance improvement. Hence the duration of the nonzero vector is achieved according to the principle of current error minimization. The issues of optimal duty Ratio, vector selection and arrangement, and control digital delay compensation are surveyed in detail.

Comprehensive simulation results are discussed to compare the performance of the proposed MPCC with the prior MPCC. It is found that, at the same sampling time, the proposed MPCC can obtain decreased current ripples and lower current THD. Therefore the presented simulation results approve the efficiency of the proposed MPCC with optimal duty cycle control.

References

[1] Almaktoof A. M., Raji A. K., & Kahn M. T., "Finite-Set Model Predictive Control and DC-Link Capacitor Voltages Balancing for Three-Level NPC Inverters", Proceeding of the 16th International Power Electronics and Motion Control Conference and Exposition (PEMC 2014), IEEE Press, Sep. 2014, pp. 224 – 229, doi: 10.1109/EPEPEMC.2014.6980716.

[2] Cara Marcy, Renewable generation capacity expected to account for most 2016 capacity additions, http://www.eia.gov/todayinenergy/detail.php?id=29492 (JAN. 2017).

[3] J. Rodriguez, B. Wu, M. Rivera, C. Rojas, V. Yaramasu , A. Wilson, "Predictive Current Control of Three-Phase Two-Level Four-Leg Inverter" 14th International Power Electronics and Motion Control Conference (EPE-PEMC), IEEE Press, Oct. 2010, pp:106-110, doi: 10.1109/EPEPEMC.2010.5606804.

[4] Jose Rodriguez, Patricio Cortes, "Predictive control of power converters and electrical drives", Wiley-IEEE Press, doi: 10.1002/9781119941446.index.

[5] P. Cortes, J. Rodriguez, P. Antoniewicz, and M. Kazmierkowski, "Direct power control of an AFE using predictive control", IEEE Trans. Power Electron, vol. 23, Sep. 2008, pp. 2516–2523, doi: 10.1109/TPEL.2008.2002065.

[6] PÁSTOR, Marek - DUDRIK, Jaroslav, "Grid-tied Multilevel Inverter With Predictive Current Control", Journal of Electrical and Electronics Engineering, vol. 5, Sep. 2013, pp. 173-178, doi: 10.7305/automatika.54-3.186 .

[7] Patricio Cortés, Gabriel Ortiz, Juan I. Yuz, José Rodríguez, Sergio Vazquez and Leopoldo G. Franquelo, "Model Predictive Control of an Inverter With Output *LC* Filter for UPS Applications" IEEE TRANSACTIONS ON INDUSTRIAL ELECTRONICS, vol. 56, Jul. 2009, pp. 1875-1883, doi: 10.1109/TIE.2009.2015750.

[8] S. Mariethoz and M. Morari, "Explicit model-predictive control of a pwm inverter with an lcl filters" IEEE Trans. Ind. Electron, vol.56, Feb. 2009, pp.389-399, doi: 10.1109/TIE.2008.2008793.

[9] Sergio Vazquez, Abraham Marquez, Ricardo Aguilera, Daniel Quevedo, Jose I. Leon and Leopoldo G. Franquelo, "Predictive Optimal Switching Sequence Direct Power Control for Grid Connected Power Converters" IEEE Transactions on Industrial Electronics, vol. 62, pp. 2010 – 2020, Apr 2015, doi: 10.1109/TIE.2014.2351378.

[10] Sung-Yeul Park, Jih-Sheng Lai, Woo-Cheol Lee, "An Easy, Simple, and Flexible Control Scheme for a Three-Phase Grid-Tie Inverter System", Energy Conversion Congress and Exposition (ECCE), IEEE Press, Nov. 2010, pp.599-603, doi: 10.1109/ECCE.2010.5617961.

[11] U.S. Energy Information Administration, EIA projects world energy consumption will increase 56% by 2040, http://www.eia.gov/todayinenergy/detail.php?id=12251 (JUL. 2013).

[12] Yongchang Zhang, Changqi Qu, Zhengxi Li, Yingchao Zhang, Longhan Cao, "Direct Power Control of PWM Rectifier With Optimal Duty Ratio Under Unbalanced Network" Power Electronics and ECCE Asia (ICPE-ECCE Asia), IEEE Press, Jun. 2015, pp.1116 - 1122, doi: 10.1109/ICPE.2015.7167920.

[13] Yongchang Zhang, Haitao Yang, "Model predictive torque control with duty ratio optimization for two-level Inverterfed induction motor drive" 2013 International Conference on Electrical Machines and Systems (ICEMS), IEEE Press, Jan. 2014, pp. 2189 - 2194, doi: 10.1109/ICEMS.2013.6713196.

[14] Yongchang Zhang, Wei Xie, Zhengxi Li and Yingchao Zhang, "Model Predictive Direct Power Control of a PWM Rectifier With Duty Cycle Optimization" IEEE Transactions on Power Electronics, vol. 28, Nov. 2013, pp. 5343-5351, doi: 10.1109/TPEL.2013.2243846.

[15] Yongchang Zhang, Yubin Peng, "Model Predictive Current Control with Optimal Duty Cycle for Three-Phase Grid-Connected AC/DC Converters" Power Electronics and Application Conference and Exposition (PEAC), IEEE Press, 2014, pp. 837 – 842, . doi: 10.1109/PEAC.2014.7037967.

[16] Yongchang Zhang, Yubin Peng, Bo Xia "Efficient model predictive control with optimal duty cycle for power converters" Power Electronics and Motion Control Conference (IPEMCECCE Asia), IEEE Press, Jul. 2016, pp. 1076 - 1083, doi: 10.1109/IPEMC.2016.7512436.

Authors

SHAHROUZ EBRAHIMPANAH received the M.Sc. degree in power electronic and drives from the School of Automation at Wuhan University of Technology, Wuhan, China, in 2015, where he is currently pursuing the Ph.D. degree in Technology of Intelligent Systems and Intelligent Control. His research interests include model predictive control for inverters.

MISBAWU ADAM received the B.S. degree in Electrical ans Electronic Engineering from the Kwame Nkrumah University of Science and Technology, Kumasi, Ghana in 2011. He receives his M.Sc. in Power Electronics and Drives from the school of Automation at Wuhan University of Technology, Wuhan, China, in 2015 where he is currently pursuing the Ph.D. degree in Traffic Information Engineering and Control in the field of Power Electronics and Drives. His research area is Active Power Filters.

QIHONG CHEN (M'08) received the Ph.D. degree in control science and engineering from Southeast University, Nanjing, China, in 2003. He is currently a Professor in the school of Automation at the Wuhan University of Technology, Wuhan, China. His current research interests include grid tied inverters and predictive control.

YUEPENG CHEN, From March 2005 to March 2008, he graduated from Northeastern University with a degree in Control Science and Engineering. From March 2007 to March 2008, he was a senior visiting scholar at the Department of Electrical and Computer Engineering at Monash University in Australia.

He is currently a Professor in the school of Automation at the Wuhan University of Technology, Wuhan, China. His current research direction include: fault diagnosis and fault-tolerant control Singular system theory and application Modeling and Algorithm Research Signal and Image Processing.